

# **Closed Form Design Equations for Strengthened Concrete Beams: FRP Rupture**

**by N. Hatami and H.A. Rasheed**

**Synopsis:** Externally bonded FRP has been established as the technology of choice to strengthen RC beams. Researchers and practicing engineers have recently developed design guidelines for FRP strengthening. However, the current state of the art flexural design procedure suggests an iterative process. No earlier efforts have been devoted to develop direct strength design equations on the failure mode of FRP rupture that can facilitate structural calculations. This study develops exact and approximate sets of closed form equations to design singly and doubly reinforced strengthened rectangular sections that fail by FRP rupture. Comparisons with reported experimental strength data indicate excellent agreement. A comprehensive parametric study has yielded a simple linear regression equation that has an almost perfect statistical correlation and is equally applicable in cases of analysis and design. Comparison between the exact solution and the regression equation confirms the accuracy of the latter. The latter is used in a design example.

**Keywords:** concrete beams; design equations; flexural strengthening; FRP rupture

## 1614 Hatami and Rasheed

**Naghme Hatami** is a graduate student in the Institute of Civil Engineering at Lund Institute of Technology, Lund, Sweden. Her research interests include reinforced concrete structures strengthened by fiber-reinforced polymer composites.

**Hayder A. Rasheed** is assistant professor of Civil Engineering at Kansas State University. He is member of ACI Committee 440-Fiber Reinforced Polymer and chair of the Stability Committee of the Engineering Mechanics Division of ASCE. His research interests include behavior of concrete structures reinforced and strengthened by fiber-reinforced polymers and stability of Composite Structural Components.

### INTRODUCTION

There is a large volume of studies in the literature addressing different behavioral aspects of FRP strengthening of reinforced concrete beams. Researchers and practitioners have recently developed design guidelines for FRP external strengthening of existing concrete structures (ISIS Canada 2001, FIB 2001, ACI 440.2R-02). However, the flexural design procedures implemented by these guidelines suggest an iterative approach. This iterative approach was extended from earlier studies (Chaallal et. al. 1998 and Saadatmanesh and Malek 1998). The three main flexural failure modes identified for FRP-strengthened beams are brittle concrete crushing (prior to steel yielding), ductile concrete crushing (after steel yielding) and FRP rupture (ACI 440.2R-02). Chaallal et. al. (1998) and Saadatmanesh and Malek (1998) addressed the ductile concrete crushing and FRP rupture modes only. Rasheed and Pervaiz (2003) developed direct non-iterative equations for the failure mode of ductile concrete crushing, which is dominant for moderately reinforced sections. On the other hand, the FRP rupture failure mode provides the highest utilization of the material and offers utmost section ductility prior to failure, due to the high tensile strength of FRP. However, it also yields a brittle catastrophic failure due to the sudden release of FRP energy upon fiber rupture. This is the dominant failure mode for lightly reinforced and flanged sections. No earlier efforts have been devoted to develop direct design equations for this failure mode that can facilitate structural calculations.

The objective of this study is to develop closed form analytical design equations for rectangular beam sections strengthened with externally bonded FRP that have a failure mode of FRP rupture. Both exact and approximate equations are derived for singly and doubly reinforced rectangular sections strengthened with flat FRP sheets. To illustrate the accuracy of the approximate equations on a wide range of results, as compared to the exact ones, an extensive parametric study is performed. This parametric study has resulted in a unique linear equation having an almost perfect statistical correlation that can be equally used in analysis or design. In cases where bond failure controls the design, the strain limit  $\kappa_m \varepsilon_{fu}$  of ACI 440.2R-02 may replace the rupture strain  $\varepsilon_{fu}$  in the present equations.

### ASSUMPTIONS

1. Reinforcing steel is assumed to have an elastic-perfectly plastic stress-strain curve.
2. Concrete response in compression is assumed to follow Hognestad's parabola (Park and Paulay 1975).
3. Since the predominant failure mode considered is FRP rupture, concrete extreme fiber strain in compression may not exceed the design level for crushing ( $\varepsilon_{cf} < 0.003$ ).
4. Concrete contribution in tension is assumed to be negligible at ultimate capacity.
5. FRP, along the fiber direction, has a linear stress-strain curve up to brittle failure.

### MAXIMUM FRP REINFORCEMENT RATIO

The equations developed in this paper are based on the FRP rupture flexural failure mode. To ensure that this mode controls the design, the FRP ratio should be kept below the balanced ratio, which would cause simultaneous concrete crushing and FRP rupture. This ratio is determined using expressions developed by Rasheed and Pervaiz (2003) for singly and doubly reinforced rectangular sections, Fig. 1:

$$\rho_f^{b \max} = \frac{A_f^{b \max}}{bd} = 0.85 \frac{f'_c}{f_{fu}} \left( \frac{a_b^{\max}}{d} \right) - \rho_s \frac{f_y}{f_{fu}} \quad (\text{singly reinforced section}) \quad (1)$$

where  $a_b^{\max} = \beta_1 c_b^{\max} = \frac{\varepsilon_{cu} h}{\varepsilon_{cu} + \bar{\varepsilon}_{fu}}$ ,  $\rho_s = \frac{A_s}{bd}$ ,  $\bar{\varepsilon}_{fu} = \varepsilon_{fu} + \varepsilon_{bi}$ ,  $\varepsilon_{fu}$  is the FRP design ultimate strain,  $\varepsilon_{bi}$  is the initial tensile strain at the bottom of the section due to pre-existing loads during strengthening,  $\varepsilon_{cu} = 0.003$  at concrete crushing.

$$\tilde{\rho}_f^{b \max} = \rho_f^{b \max} + \rho'_s \frac{f'_s{}^{b \max}}{f_{fu}} \quad (\text{doubly reinforced section}) \quad (2)$$

where

$$f_s'^{b\max} = \begin{cases} f_y & \text{if } \frac{d'}{h} \leq \frac{600 - f_y}{600 + 200000\bar{\epsilon}_{fu}} \text{ (SI)} \\ & \text{or } \frac{d'}{h} \leq \frac{87 - f_y}{87 + 29000\bar{\epsilon}_{fu}} \text{ (US)} \\ 600 - \frac{d'}{h}(600 + 200000\bar{\epsilon}_{fu}) \text{ (SI)} & , \text{ otherwise} \\ \text{or } 87 - \frac{d'}{h}(87 + 29000\bar{\epsilon}_{fu}) \text{ (US)} & \end{cases}$$

**DIRECT DESIGN EQUATIONS FOR FRP RUPTURE**

**Parameters for the nonlinear concrete model**

As stated earlier, Hognestad’s parabola is used to model the concrete stress-strain relationship in compression.

$$\sigma_c = f_c' \left[ 2 \frac{\epsilon_c}{\epsilon_c'} - \left( \frac{\epsilon_c}{\epsilon_c'} \right)^2 \right] \tag{3}$$

where  $f_c'$  is the compressive strength of concrete and  $\epsilon_c'$  is the strain corresponding to  $f_c'$ . Based on Hogenstad’s parabola, the  $\alpha$  factor is used to convert the non-linear stress-strain relationship into an equivalent rectangular distribution (Park and Paulay 1975).

$$\alpha = \frac{\int_0^{\epsilon_{cf}} \sigma_c d\epsilon_c}{f_c' \epsilon_{cf}} = \frac{\epsilon_{cf}}{\epsilon_c'} - \frac{\epsilon_{cf}^2}{3\epsilon_c'^2} \tag{4}$$

where  $\epsilon_{cf}$  is the concrete extreme fiber compressive strain at FRP rupture. This strain ( $\epsilon_{cf}$ ) is expressed in terms of the FRP ultimate rupture strain using the following strain compatibility equation:

$$\frac{\epsilon_{cf}}{c_n} = \frac{\bar{\epsilon}_{fu}}{h - c_n} \Rightarrow \epsilon_{cf} = \frac{\bar{\epsilon}_{fu} c_n}{h - c_n} \tag{5}$$

where  $\bar{\epsilon}_{fu} = \epsilon_{fu} + \epsilon_{bi}$ ,  $\epsilon_{fu}$  is the design ultimate strain of the FRP,  $\epsilon_{bi}$  is the initial tensile strain at the bottom of the section due to pre-existing loads during strengthening. Substituting Equation (5) into Equation (4), the parameter  $\alpha$  is written in terms of the depth of neutral axis ( $c_n$ ):

$$\alpha = \frac{\bar{\varepsilon}_{fu} c_n}{(h - c_n) \varepsilon'_c} - \frac{(\bar{\varepsilon}_{fu} c_n)^2}{3(h - c_n)^2 \varepsilon'_c{}^2} \quad (6)$$

The point of action of the compressive force of concrete  $C$ , measured from the extreme compression fiber of concrete, is written as a fraction of the neutral axis depth ( $\gamma c_n$ ). The expression for  $\gamma$  is derived as follows, (Park and Paulay 1975):

$$\gamma = 1 - \frac{\int_0^{\varepsilon_{cf}} \varepsilon_c \sigma_c d\varepsilon_c}{\varepsilon_{cf} \int_0^{\varepsilon_{cf}} \sigma_c d\varepsilon_{cf}} = \frac{1 - \frac{\varepsilon_{cf}}{12\varepsilon'_c}}{1 - \frac{\varepsilon_{cf}}{3\varepsilon'_c}} \quad (7)$$

Substituting Equation (5) into Equation (7), the parameter  $\gamma$  is written in terms of the depth of neutral axis ( $c_n$ ):

$$\gamma = \frac{4\varepsilon'_c h - c_n(4\varepsilon'_c + \bar{\varepsilon}_{fu})}{12\varepsilon'_c h - c_n(12\varepsilon'_c + 4\bar{\varepsilon}_{fu})} \quad (8)$$

### Exact solution for singly reinforced rectangular sections

Strength of reinforced concrete sections is accurately determined if strain compatibility and force equilibrium equations are simultaneously solved by imposing the constitutive relationships. The force equilibrium equation, at FRP rupture condition, for the singly reinforced section is:

$$\sum F_x = 0 \Rightarrow \alpha f'_c b c_n - A_s f_y - A_f f_{fu} = 0 \quad (9)$$

The moment equilibrium equation about the centroid of FRP plate is:

$$\bar{M}_u = \phi \bar{M}_n = \phi \alpha f'_c b c_n (d_f - \gamma c_n) - \phi A_s f_y (d_f - d) \quad (10)$$

where  $\bar{M}_u$  is the ultimate design moment of the strengthened section,  $\phi=0.9$  is the strength reduction factor as defined by ACI 440.2R-02,  $\bar{M}_n$  is the nominal moment capacity of the strengthened section,  $A_s$  is the tension steel reinforcement in the section,  $d$  is the effective depth from the top of the section to the centroid of  $A_s$  and  $d_f$  is the depth from the top of the section to the centroid of FRP.  $d_f$  is assumed to approximately equal the section depth ( $h$ ) since the FRP plate thickness is negligible compared to  $h$  and it is unknown in design problems. The concrete strain  $\varepsilon_{cf}$  is related to the FRP rupture strain

## 1618 Hatami and Rasheed

using the strain compatibility, Equation (5). By re-arranging the moment equilibrium expression, Equation (10), above:

$$\frac{\bar{M}_u}{\phi f'_c b h^2} = \frac{\bar{M}_n}{f'_c b h^2} = \frac{\alpha c_n (h - \gamma c_n)}{h^2} - \rho_s \frac{f_y}{f'_c} \frac{d}{h} \left(1 - \frac{d}{h}\right) \quad (11)$$

where  $\rho_s = \frac{A_s}{bd}$ . Grouping the second term on the right hand side with the left hand side term as  $Q_u$ , Equation (11) above becomes:

$$Q_u - \frac{\alpha c_n (h - \gamma c_n)}{h^2} = 0 \quad (12)$$

$$\text{where } Q_u = \frac{\bar{M}_n}{f'_c b h^2} + \rho_s \frac{f_y}{f'_c} \frac{d}{h} \left(1 - \frac{d}{h}\right)$$

Substituting the  $\alpha$  and  $\gamma$  expressions, Equations (6) and (8), into Equation (12), and manipulating the tedious algebraic operations, the following exact 5<sup>th</sup> degree polynomial, in terms of the normalized depth of the neutral axis ( $c_n$ ), is obtained:

$$A \frac{c_n}{h} + B \left(\frac{c_n}{h}\right)^2 + D \left(\frac{c_n}{h}\right)^3 + E \left(\frac{c_n}{h}\right)^4 + F \left(\frac{c_n}{h}\right)^5 - 12 Q_u \varepsilon'_c = 0 \quad (13)$$

where

$$A = Q_u (4\bar{\varepsilon}_{fu} + 36\varepsilon'_c)$$

$$B = \bar{\varepsilon}_{fu} (12 - 8Q_u) - 36Q_u \varepsilon'_c$$

$$D = -28\bar{\varepsilon}_{fu} - 8 \frac{(\bar{\varepsilon}_{fu})^2}{\varepsilon'_c} + Q_u (12\varepsilon'_c + 4\bar{\varepsilon}_{fu})$$

$$E = \bar{\varepsilon}_{fu} \left(20 + \frac{31\bar{\varepsilon}_{fu}}{3\varepsilon'_c} + \frac{4(\bar{\varepsilon}_{fu})^2}{3(\varepsilon'_c)^2}\right)$$

$$F = -\frac{\bar{\varepsilon}_{fu}}{\varepsilon'_c} (4\varepsilon'_c + \bar{\varepsilon}_{fu}) \left(1 + \frac{\bar{\varepsilon}_{fu}}{3\varepsilon'_c}\right)$$

Solving Equation (13) above for its lowest positive root yields the value of  $c_n$ . By using the force equilibrium, Equation (9), the amount of FRP reinforcement is consequently determined. The ratio for FRP reinforcement is:

$$\rho_f = \alpha \frac{f'_c}{f_{fu}} \left(\frac{c_n}{d}\right) - \rho_s \frac{f_y}{f_{fu}} \quad (14)$$

where  $\rho_f = \frac{A_f}{bd}$

### Exact solution for doubly reinforced rectangular sections

Doubly reinforced sections have both tension and compression reinforcement. The main complication in design occurs when the compression steel is located close enough to the neutral axis such that it does not yield at rupture failure. Both cases, where the compression reinforcement yields and does not yield, are presented in this paper.

The force equilibrium equation, at FRP rupture condition, for a doubly reinforced section is:

$$\sum F_x = 0 \Rightarrow \alpha f'_c bc_n - A_s f_y - A_f f_{fu} + A'_s f'_s = 0 \quad (15)$$

As for the singly reinforced section, the moment equilibrium is taken about the centroid of the FRP plate:

$$\bar{M}_u = \phi \alpha f'_c bc_n (d_f - \gamma c_n) - \phi A_s f_y (d_f - d) + \phi A'_s f'_s (d_f - d') \quad (16)$$

where  $A'_s$  is the compression steel reinforcement in the section and  $d'$  is the top cover depth to the centroid of  $A'_s$ ,  $d_f$  is replaced with  $h$  as justified above,  $f'_s$  is the stress in compression steel related to the FRP rupture strain using strain compatibility, as follows, Fig. 1:

$$\varepsilon'_s = \bar{\varepsilon}_{fu} \left( \frac{c_n - d'}{h - c_n} \right) \quad (17)$$

Accordingly, a verification calculation must be done to check whether the compression steel will yield or not. Since it is typically assumed that the compression steel will always yield first hand,  $f_y$  is substituted, in the trial attempt, for the stress in the compression reinforcement ( $f'_s$ ).

Yielding of compression reinforcement-- Invoking Equation (16) and rearranging its terms:

$$\frac{\bar{M}_u}{\phi f'_c b h^2} = \frac{\bar{M}_n}{f'_c b h^2} = \frac{\alpha c_n (h - \gamma c_n)}{h^2} - \rho_s \frac{f_y}{f'_c} \frac{d}{h} \left(1 - \frac{d}{h}\right) + \rho'_s \frac{f_y}{f'_c} \frac{d}{h} \left(1 - \frac{d'}{h}\right) \quad (18)$$

where  $\rho'_s = \frac{A'_s}{bd}$ . Grouping the  $Q_u$  term, defined earlier, with the third term on the right hand side as  $Q'_u$ , Equation (18) above becomes:

$$Q'_u - \frac{\alpha c_n (h - \gamma c_n)}{h^2} = 0 \quad (19)$$

## 1620 Hatami and Rasheed

where  $Q'_u = Q_u - \rho'_s \frac{f_y}{f'_c} \frac{d}{h} \left(1 - \frac{d'}{h}\right)$ .

Substituting Equations (6) and (7) into (19) and manipulating the tedious algebraic steps, Equation (19) will give the 5<sup>th</sup> degree polynomial needed to exactly solve for the neutral axis depth ( $c_n$ ):

$$A' \frac{c_n}{h} + B' \left(\frac{c_n}{h}\right)^2 + D' \left(\frac{c_n}{h}\right)^3 + E' \left(\frac{c_n}{h}\right)^4 + F' \left(\frac{c_n}{h}\right)^5 - 12Q'_u \varepsilon'_c = 0 \quad (20)$$

where

$$A' = Q'_u (4\bar{\varepsilon}_{fu} + 36\varepsilon'_c) \quad , \quad E' = E$$

$$B' = \bar{\varepsilon}_{fu} (12 - 8Q'_u) - 36\varepsilon'_c Q'_u \quad , \quad F' = F$$

$$D' = -28\bar{\varepsilon}_{fu} - 8 \frac{\bar{\varepsilon}_{fu}^2}{\varepsilon'_c} + Q'_u (12\varepsilon'_c + 4\bar{\varepsilon}_{fu})$$

No yielding of the compression reinforcement-- When  $\varepsilon'_s < \varepsilon_y$ , the compression steel will not yield at FRP rupture. Therefore, the stress in the compressive reinforcement is calculated as  $f'_s = \varepsilon'_s E_s$ . The moment equation will slightly change as follows:

$$\frac{\bar{M}_u}{\phi f'_c b h^2} = \frac{\bar{M}_n}{f'_c b h^2} = \frac{\alpha c_n (h - \gamma c_n)}{h^2} - \rho_s \frac{f_y}{f'_c} \frac{d}{h} \left(1 - \frac{d}{h}\right) + \rho'_s \frac{\varepsilon'_s E_s}{f'_c} \frac{d}{h} \left(1 - \frac{d'}{h}\right) \quad (21)$$

Re-writing Equation (29) in terms of  $Q_u$ :

$$Q_u - \frac{\alpha c_n (h - \gamma c_n)}{h^2} - \rho'_s \frac{\varepsilon'_s E_s}{f'_c} \frac{d}{h} \left(1 - \frac{d'}{h}\right) = 0 \quad (22)$$

Substituting Equations (6), (7) and (17) into (22) and manipulating the tedious algebraic steps, Equation (22) will give the 5<sup>th</sup> degree polynomial needed to exactly solve for the neutral axis depth ( $c_n$ ):

$$A'' \frac{c_n}{h} + B'' \left(\frac{c_n}{h}\right)^2 + D'' \left(\frac{c_n}{h}\right)^3 + E'' \left(\frac{c_n}{h}\right)^4 + F'' \left(\frac{c_n}{h}\right)^5 - 12\varepsilon'_c \left(Q_u + G \frac{d'}{h}\right) = 0 \quad (23)$$

where

$$A'' = A + G(12\varepsilon'_c(1 + 2\frac{d'}{h}) + 4\bar{\varepsilon}_{fu} \frac{d'}{h})$$

$$B'' = B - G(12\varepsilon'_c(2 + \frac{d'}{h}) + 4\bar{\varepsilon}_{fu}(1 + \frac{d'}{h}))$$

$$D'' = D + G(12\varepsilon'_c + 4\bar{\varepsilon}_{fu})$$

$$E'' = E$$

$$F'' = F$$

$$G = \rho'_s \frac{E_s \bar{\varepsilon}_{fu}}{f'_c} \frac{d}{h} (1 - \frac{d'}{h})$$

Determining FRP reinforcement ratio-- The ratio of FRP reinforcement is simply calculated for the doubly reinforced section by using the force equilibrium, Equation (15), after obtaining  $c_n$  from Equation (20) or (23).

$$\rho_f = \alpha \frac{f'_c}{f_{fu}} (\frac{c_n}{h}) - \rho_s \frac{f_y}{f_{fu}} + \rho'_s \frac{f_y}{f_{fu}} \quad (24)$$

### Approximate solution for singly reinforced rectangular sections

The 5<sup>th</sup> degree polynomial equations above can be simplified using rational approximate expressions for the  $\alpha$  and  $\gamma$  factors in Equations (4) and (8). The concrete strain corresponding to  $f'_c$  ( $\varepsilon'_c$ ) is closely approximated by 0.002 for normal and moderately high strength concrete. Substituting the constant value of  $\varepsilon'_c$  into Equations (4) and (8),  $\alpha$  and  $\gamma$  can be expressed in terms of  $\varepsilon_{cf}$  as follows:

$$\alpha = 500\varepsilon_{cf} - 83333\varepsilon_{cf}^2 \quad (25)$$

$$\gamma = \frac{0.33 - 41.67\varepsilon_{cf}}{1 - 166.67\varepsilon_{cf}} \quad (26)$$

The  $\gamma$  expression in Equation (26) is significantly simplified by a linear  $\gamma$  regression function of  $\varepsilon_{cf}$  generated with an excellent coefficient of correlation ( $R^2=0.9677$ ), see Fig. 2:

$$\gamma = 27.768\varepsilon_{cf} + 0.3239 \quad (27)$$

Equation (25) still presents no simplification for the  $\alpha$  expression. Observing the discrete  $\alpha$  points on Fig. 3, one may notice that the parabolic curve may be approximated by two straight lines with a breaking point at around  $\varepsilon_{cf}=0.0015$ . Fitting the two ranges

## 1622 Hatami and Rasheed

of  $\varepsilon_{cf}$  by two least square lines, the following approximate equations are generated for  $\alpha$  with excellent coefficients of correlation ( $R^2=0.9931$  and  $0.9305$  respectively), Fig. 3:

$$\alpha = 366.67\varepsilon_{cf} + 0.0417 \quad 0 \leq \varepsilon_{cf} < 0.0015 \quad (28)$$

$$\alpha = 125\varepsilon_{cf} + 0.4042 \quad 0.0015 \leq \varepsilon_{cf} \leq 0.003 \quad (29)$$

In addition, the values of  $\gamma$  in Fig. 2 are seen to have a slight variation along the entire range of  $\varepsilon_{cf}$ . Accordingly, Equation (27) may be further simplified by considering two constant values of  $\gamma$  for the two ranges of strain identified above in the case of  $\alpha$ . These constant values are selected to be the average of the two end values of each strain range:

$$\gamma = \frac{\gamma_0 + \gamma_{0.0015}}{2} = 0.3447 \quad 0 \leq \varepsilon_{cf} \leq 0.0015 \quad (30)$$

$$\gamma = \frac{\gamma_{0.0015} + \gamma_{0.003}}{2} = 0.3864 \quad 0.0015 \leq \varepsilon_{cf} \leq 0.003 \quad (31)$$

By substituting Equations (28)-(31) into the moment equilibrium, Equation (12), a 3<sup>rd</sup> degree approximate polynomial equation will be developed:

$$A_3 \frac{c_n}{h} + B_3 \left(\frac{c_n}{h}\right)^2 + D_3 \left(\frac{c_n}{h}\right)^3 - Q_u = 0 \quad (32)$$

where

For  $\varepsilon_{cf} \leq 0.0015$ :

$$A_3 = 0.0417 + Q_u$$

$$B_3 = 366.67\bar{\varepsilon}_{fu} - 0.056$$

$$D_3 = -126.4\bar{\varepsilon}_{fu} + 0.0144$$

For  $0.0015 < \varepsilon_{cf} \leq 0.003$ :

$$A_3 = 0.4042 + Q_u$$

$$B_3 = 125\bar{\varepsilon}_{fu} - 0.560$$

$$D_3 = -48.3\bar{\varepsilon}_{fu} + 0.156$$

The approximate equations are easier to apply than the exact ones and can be directly solved for  $c_n$  using a scientific calculator. Once  $c_n$  is determined, the ratio of FRP reinforcement is directly obtained from Equation (14).

### Approximate solution for doubly reinforced section

As for singly reinforced sections, the same approximations are applied for this case. The approximate equations are expressed in terms of the yielding status of compression reinforcement, as presented earlier:

Yielding of compression steel-- The cubic equation of  $c_n$  changes to:

$$A_3 \frac{c_n}{h} + B_3 \left(\frac{c_n}{h}\right)^2 + D_3 \left(\frac{c_n}{h}\right)^3 - Q'_u = 0 \quad (33)$$

where  $A_3$ ,  $B_3$ ,  $D_3$  are defined above and  $Q'_u$  is defined earlier in the exact solution, Equation (19).

No yielding of compression steel-- The cubic equation in  $c_n$  becomes:

$$A'_3 \frac{c_n}{h} + B'_3 \left(\frac{c_n}{h}\right)^2 + D'_3 \left(\frac{c_n}{h}\right)^3 - Q_u h - Gd' = 0 \quad (34)$$

where

$$A'_3 = A_3 + G$$

$$B'_3 = B_3$$

$$D'_3 = D_3$$

$G$  is defined under Equation (23).

The approximate Equations (33) or (34) are easier to solve for  $c_n$ , as the smallest positive root, using a scientific calculator. The FRP reinforcement ratio for doubly reinforced sections is directly calculated using the Equation (24).

## EXPERIMENTAL VERIFICATION

A total of 9 FRP-strengthened reinforced concrete beams, with a variety of properties, tested by others are used to verify the equations developed in this paper, Table 1. All of these beams have failed in FRP rupture and are therefore chosen for comparison.

The results obtained from the exact solution, Equations (13)-(14), (20) or (23) and (24), are compared to those of the approximate solution, Equations (32)-(34), and to the experimental values, Fig. 4 and 5.

It can be seen from Figs. 4 and 5 that the comparison yields an almost perfectly matching results for  $c_n$  and  $\rho_f$ . This provides confidence in the accuracy of the exact equations and in the validity of the assumptions adopted for the approximate solution, for the range of experimental data examined.

## PARAMETRIC STUDY

To examine the relevance of the approximate solution to the exact one, an extensive parametric study is conducted. This study was also done to investigate the effects of the design variables on the results. These variables are the cross section dimensions, tension steel reinforcement ratio, compression steel reinforcement ratio, strengthening design moment, concrete material properties, steel material properties, FRP material type and properties, as shown in Fig. 6.

## 1624 Hatami and Rasheed

For every set of fixed variables, the FRP ratio is set to zero first and the moment of the unstrengthened beam is calculated ( $M_n$ ). The moment of strengthened beam ( $\bar{M}_n$ ) is then increased by  $0.1M_n$  steps ( $1.1M_n, 1.2M_n, \dots$ ) and the corresponding FRP ratio is calculated until the mode of failure changes from FRP rupture to concrete crushing. Steel ratios close to the maximum limit always yields concrete crushing failure mode. Accordingly, the tension steel ratio is limited to three values varying from minimum to moderately high levels (0.0045, 0.00875, and 0.013). The compression steel is varied between zero (singly reinforced section), a low ratio (0.002) and a high ratio (0.01). The two FRP materials examined are Glass FRP (GFRP) and carbon FRP (CFRP). The GFRP is assumed to have a modulus of elasticity of  $E_{GFRP} = 45$  GPa and a strength of  $f_{GFRP} = 400$  MPa. The CFRP properties are assumed to be  $E_{CFRP} = 400$  GPa and  $f_{CFRP} = 3000$  MPa.

The results were individually plotted in terms of the relationship between the ratio of strengthened to unstrengthened moment capacity  $\bar{M}_n/M_n$  vs. the FRP ratio. These results were studied to investigate the effects of changing the variables. The plots are not shown here for space limitation reasons but they are presented in Hatami (2004).

The results have shown that the FRP ratio is always a linear function of the ratio of moment capacity. Some of the design variables have a direct effect in changing the slope of this linear relationship and the rest of the variables have no such influence. The tension steel ratio ( $\rho_s$ ), the ultimate strength of FRP ( $f_{fu}$ ) and the yielding strength of steel ( $f_y$ ) are found to affect the slope of the resulting straight line. On the other hand, the concrete strength ( $f'_c$ ), the section geometry ratio ( $b/h$ ) and the compression steel ratio ( $\rho'_s$ ) are seen not to affect the straight-line relationship.

By normalizing the ratio of FRP, which is calculated from Equations (14) or (24), by the factors influencing the results, a unique linear variation is obtained, which can be used for any singly or doubly reinforced rectangular section. The  $\rho_f$  normalizing factor is non-dimensional and is referred to in this paper as the reinforcement strength ratio  $\lambda$ .

$$\lambda = \frac{\rho_f f_{fu}}{\rho_s f_y} \quad (35)$$

Normalizing all the FRP ratios calculated for the parametric study to obtain the corresponding  $\lambda$  values and plotting it against  $\bar{M}_n/M_n$ , an almost perfect straight line is generated with  $R^2 = 0.9994$ , for the 516 data points examined, Fig. 7. This presents an excellent contribution of this paper since a single linear function may be effectively used to replace the exact or approximate solutions. It can be further used to solve analysis problems as well.

$$\lambda = 0.9527 \overline{M_n} / M_n - 0.9691 \quad (36)$$

It can be further seen from Fig. 7 that all the data points with the same  $\overline{M_n} / M_n$  give the same values of  $\lambda$ .

### **Comparison of regression equation and exact solution**

To verify the accuracy of the linear regression expression, 70 different examples of the parametric study were solved again using the exact solution and the regression equation. The ratios of FRP calculated from both solutions are compared and plotted in Fig. 8. The comparison clearly presents an almost perfect match of the results. Detailed input values and results of the 70 examples solved for FRP laminates are presented in appendix B of Hatami (2004).

### **DESIGN EXAMPLE**

An example from the parametric study is selected to show the strengthening design of a beam having an FRP rupture failure mode. The example is a singly reinforced rectangular section with a width  $b = 300$  mm, a height  $h = 400$  mm and an effective height  $d = 347.5$  mm. The steel ratio  $\rho_s = 0.013$ , the strength of the concrete  $f'_c = 50$  MPa and the strength for the steel  $f_y = 350$  MPa. The section is to be strengthened with GFRP ( $E_f = 45$  GPa,  $f_{fu} = 400$  MPa). The ratio of strengthened to unstrengthened moment capacity is chosen to be  $\overline{M_n} / M_n = 1.5$ . The initial substrate strain ( $\varepsilon_{bi}$ ) is assumed to be zero.

### **Design calculations**

First, the maximum FRP ratio is calculated to confirm the governing failure mode ( $a_b^{\max} = 100.9$  mm,  $\rho_f^{b^{\max}} = 0.0195$ ). By using Equation (36),  $\lambda = 0.46$ . The FRP ratio for this section is calculated for  $f_y = 350$  MPa,  $f_{fu} = 400$  MPa,  $\rho_s = 0.013$  ( $\rho_f = 0.005232$ ), which gives an error of only 0.72 % compared to the exact solution. The governing failure mode is confirmed to be FRP rupture since  $\rho_f < \rho_f^{b^{\max}}$ . Solving for the thickness of FRP,  $t_f = 1.818$  mm, when  $b_f = 300$  mm.

### **CONCLUSIONS**

In this study, exact and approximate sets of closed form equations are developed to design singly and doubly reinforced strengthened rectangular sections that fail by FRP rupture. The accuracy of these equation sets is verified against some reported experimental strength data. A comprehensive parametric study has yielded straight-line relationships between the value of FRP ratio and the ratio of the moment capacity of strengthened to unstrengthened section. The design parameters, found to affect the slope of this linear relationship, are the steel ratio, the steel yield strength and the FRP rupture strength. The other design parameters are seen not to influence this linearity.

## 1626 Hatami and Rasheed

Accordingly, a strength ratio ( $\lambda$ ) is introduced by normalizing the FRP ratio by the parameters affecting the slope of the linear trend. As a result, this strength ratio is found to have a unique linear variation with the ratio of moment capacity of strengthened to unstrengthened section yielding a simple linear regression equation that has an almost perfect statistical correlation and is equally applicable in cases of analysis and design. Comparison between the exact solution and the regression equation confirms the accuracy of the latter. The regression equation is found to be unique regardless of the various design parameters involved. It is, therefore, used in an illustrative design example.

### ACKNOWLEDGMENTS

The authors would like to acknowledge the Department of Structural Engineering at Lund Institute of Technology in Sweden and the Department of Civil Engineering at Kansas State University in USA for supporting this collaborative effort.

### REFERENCES

ACI 440.2R-02 (2002), "Guide for the Design and Construction of Externally Bonded FRP Systems for Strengthening Concrete Structures," ACI Committee 440, American Concrete Institute, Farmington Mills, MI, 45 p.

Arduini, M., Tommaso, A., and Nanni, A., 1997, "Brittle Failure in FRP Plate and Sheet Bonded Beams," *ACI Structural Journal*, V.94, No. 4, pp. 363-370.

Chaallal, O., Nollet, M.-J. and Perraton, D. (1998) " Strengthening of Reinforced Concrete Beams with Externally Bonded Fiber-Reinforced-Plastic-Plates: Design Guidelines for Shear and Flexure," *Canadian Journal of Civil Engineering*, Vol. 25, 692-704.

Chajes, M.J.; Thomson, T.A.; Januszka T.F., (1994). "Flexural Strengthening of Concrete beams Using Externally Bonded Composite Materials" *Journal of Construction and Building Materials*, V.8, No.3, pp. 191-201.

Djelal, C., David, E., and Buyle-Bodin, F. (1996). "Utilisation de plaques en composite pour la reparation de poutres en beton arme endommagees" Proc. *2nd Conf. On Advanced Compos. Mat. In Bridges and Struct.* M. El-Badry, ed., Canadian Society for Civil Engineering, Ottawa, pp. 581-588.

FIB, 2001, "Externally Bonded FRP Reinforcement for RC Structures," *Technical report committee 9.3*, Federation Internationale Du Beton, 130 p.

Hatami, N. (2004) "Externally Bonded Fiber-Reinforced Polymers for Flexural Strengthening of Concrete Beams: Rupture Failure Mode," M.S. thesis report, Lunds Institute of Technology and Kansas State University, Rapport TVBK-5123, ISSN 0349-4969, 62 p.

ISIS Canada (2001) "Design Manual 4: Strengthening Reinforced Concrete Structures with Externally-Bonded Fiber Reinforced Polymers," The Canadian Network of Centers of Excellence on Intelligent Sensing for Innovative Structures, University of Manitoba, Winnipeg, Manitoba, Canada, Sept. 2001, 207 p.

Park, R., and Paulay, T., (1975). "Reinforced Concrete Structures," *John Wiley and Sons, Inc.*, New York, N.Y., 769 p.

Rasheed, H. A. and Pervaiz S. (2003) "Closed Form Design Equations for Flexural Strengthening of RC Beams," *Composites Part B: Engineering*, Vol. 34, No. 6, Sept., pp. 539-550.

Ritchie, A. P.; Thomas, D. A.; Lu, L.; Conelly, G. M., (1991). "External Reinforcement of Concrete Beams Using Fiber Reinforced Plastics" *ACI Structural Journal*, V. 88, No. 4, pp. 490-500.

Saadatmanesh, H. and Malek, A. M. (1998) "Design Guidelines for Flexural Strengthening of RC Beams with FRP Plates," *Journal of Composites for Construction*, Vol. 2, No. 4, pp. 158-164.

Sharif, A., Al-Sulaimani, G. J., Basunbul, I.A., Baluch, M. H., Ghaleb, B. N. (1994). "Strengthening of Initially Loaded Reinforced Concrete Beams using FRP Plates". *ACI Structural Journal*, 91(2), pp. 160-168.

Triantafillou R.C. and Plervis, N. (1992). "Strengthening of RC beams with epoxy-bonded fiber-composite materials". *Mat. and Struct.*, 25, pp. 201-211.

**Table 1— Properties of the beams used in the experimental verification.**

Beam (Reference)	FRP type	$E_f$ (GPa)	$f_{fu}$ (MPa)	$b_f$ (mm)	$t_f$ (mm)	$A_s$ (mm <sup>2</sup> )	$A'_s$ (mm <sup>2</sup> )	$f_y$ (MPa)	$f'_c$ (MPa)	$b$ (mm)	$h$ (mm)	$d$ (mm)
B2 <sup>1</sup>	C	400	3000	300	0.17	398	265	340	30	300	400	350
E3 <sup>2</sup>	G	13	138	127	1.42	71	0	413	42.5	127	75.8	50.8
G3 <sup>2</sup>	G	22	190	127	1.22	71	0	413	36	127	75.8	50.8
P4 <sup>3</sup>	G	11.7	55	150	3	308	308	500	35	150	300	270
E <sup>4</sup>	G	11.7	161	154	4.76	258	0	432	47	152	305	251
L <sup>4</sup>	C	54.4	613	152	1.27	258	0	432	43	152	305	251
P1 <sup>5</sup>	G	15.5	170	100	1	168	57	450	37.7	150	150	114
2 <sup>6</sup>	C	186	1450	42.6	0.2	33.2	0	517	44.7	76	127	111
3 <sup>6</sup>	C	186	1450	60.5	0.2	33.2	0	517	44.7	76	127	111

<sup>1</sup>Arduini et al (1997), <sup>2</sup>Chajes et al (1994), <sup>3</sup>Djelal et al. (1996), <sup>4</sup>Ritchie et al (1991), <sup>5</sup>Sharif et al (1994), <sup>6</sup>Triantafillou and Plervis (1992)

# 1628 Hatami and Rasheed

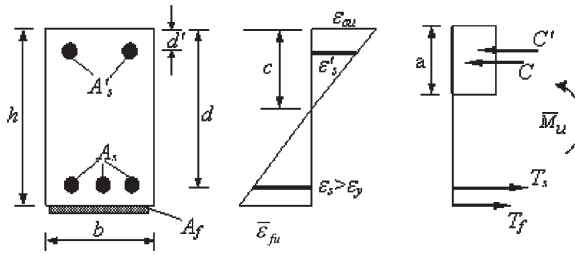


Figure 1 – Doubly reinforced cross section with strain distribution and force profile at balanced failure

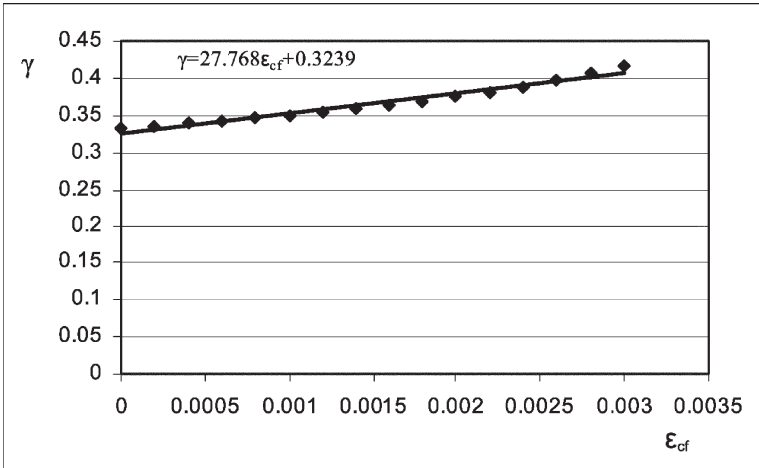


Figure 2 – Linear regression plot of  $\gamma$  vs.  $\epsilon_{cf}$  relationship

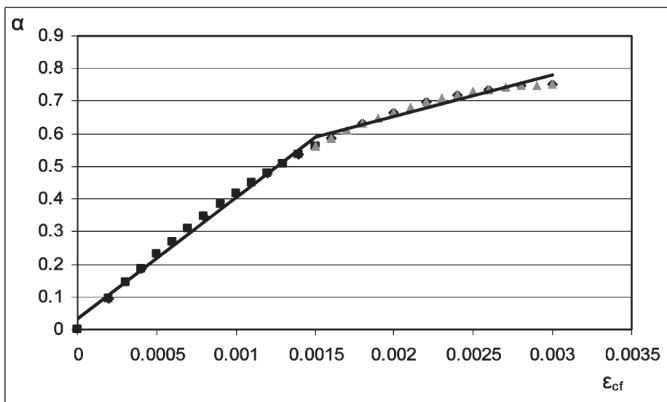
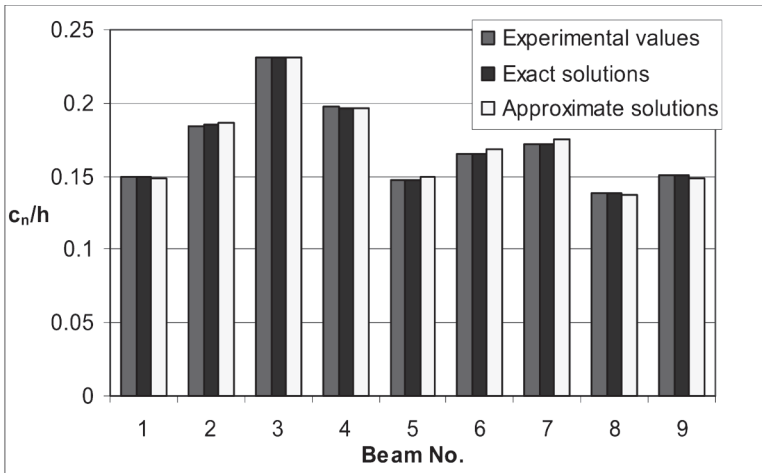
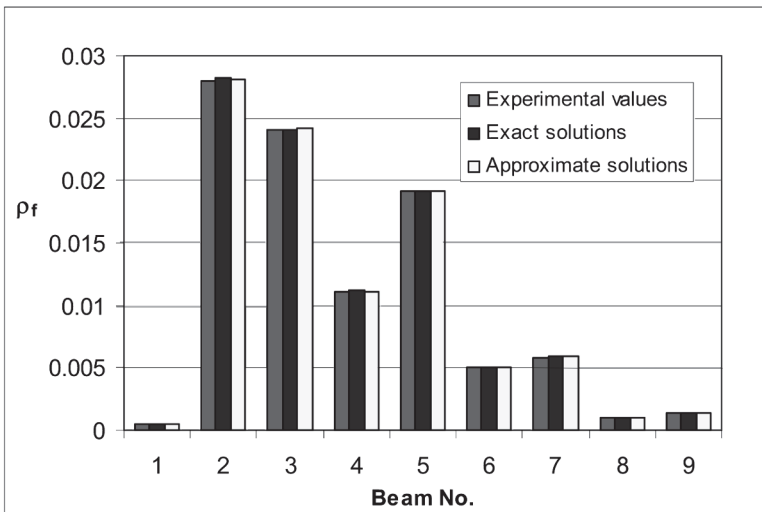


Figure 3 – Linear regression relationships of  $\alpha$  vs.  $\epsilon_{cf}$ .

Figure 4 — Experimental verification for  $c_n$  valuesFigure 5— Experimental verification for  $\rho_f$  values

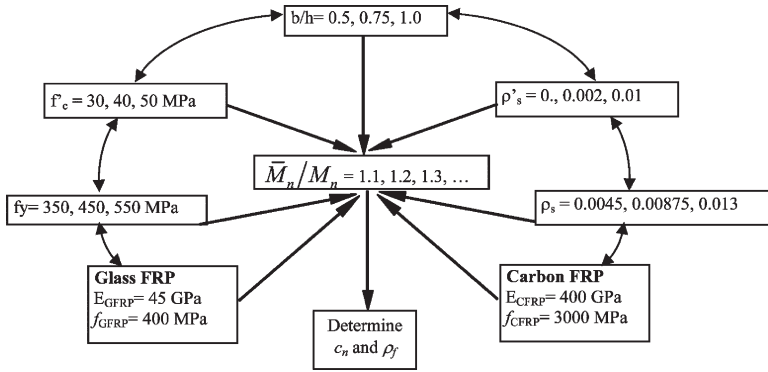


Figure 6 – Variation of design variables in the parametric study

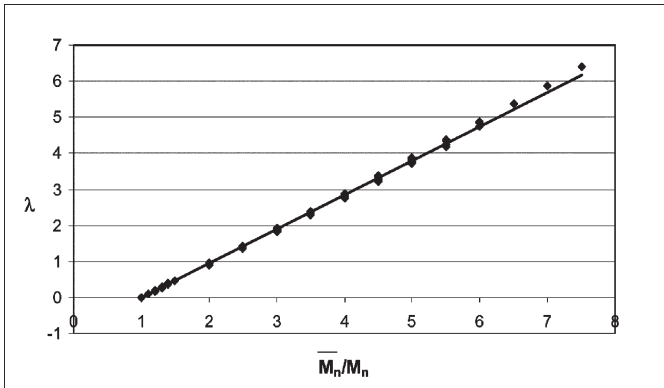


Figure 7 – The unique linear regression design equation

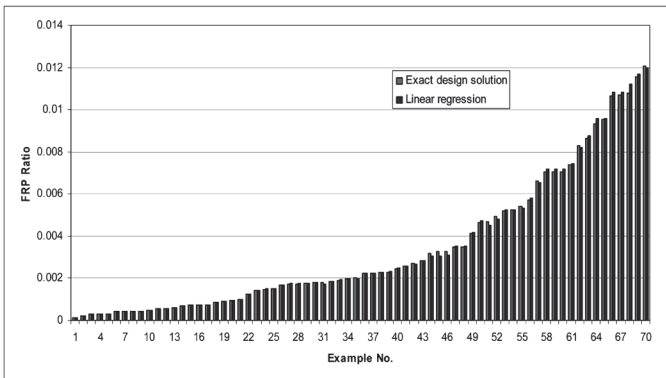


Figure 8 – Comparing the linear regression results and the exact design solution